Ion injection optimization for a linear Paul trap to study intense beam propagation

Moses Chung, Erik P. Gilson, Mikhail Dorf, Ronald C. Davidson, Philip C. Efthimion, and Richard Majeski
Plasma Physics Laboratory, Princeton University, Princeton, New Jersey 08543, USA
(Received 7 September 2006; published 26 January 2007)

The Paul Trap Simulator Experiment (PTSX) is a linear Paul trap whose purpose is to simulate the nonlinear transverse dynamics of intense charged particle beam propagation in periodic-focusing quadrupole magnetic transport systems. Externally created cesium ions are injected and trapped in the long central electrodes of the PTSX device. In order to have well-matched one-component plasma equilibria for various beam physics experiments, it is important to optimize the ion injection. From the experimental studies reported in this paper, it is found that the injection process can be optimized by minimizing the beam mismatch between the source and the focusing lattice, and by minimizing the number of particles present in the vicinity of the injection electrodes when the injection electrodes are switched from the fully oscillating voltage waveform to their static trapping voltage.

DOI: 10.1103/PhysRevSTAB.10.014202 PACS numbers: 41.85.Ar, 29.27.−a, 52.27.Jt, 52.59.Sa

I. INTRODUCTION

A fundamental understanding of intense beam propagation over long equivalent distances is important for the design and operation of modern high-intensity linear accelerators and beam transport lines [1,2]. These accelerators and transport systems are key scientific tools for various applications such as coherent radiation generation, heavy ion fusion, ion-beam-driven high-energy density physics, nuclear waste transmutation, and spallation neutron sources, to mention a few examples [1]. Recently, Davidson *et al.* [3] and Okamoto *et al.* [4] proposed a compact linear Paul trap configuration to study intense beam propagation by showing that, for certain operating conditions, the transverse dynamics of a one-component plasma trapped in the linear Paul trap is fully equivalent to that of an intense beam propagating through a periodic-focusing quadrupole magnetic field configuration. This idea has also been applied to crystalline beams in storage rings by Kjærgaard *et al.* [5]. Based on this concept, several experimental projects have been proposed and performed [6–8]. At the Princeton Plasma Physics Laboratory (PPPL), the Paul Trap Simulator Experiment (PTSX) was constructed, and successfully demonstrated quiescent beam propagation over equivalent distances of tens of kilometers, and accessed a wide operating range with stable confinement of the charge bunch [7]. The PTSX device is a long linear Paul trap with cylindrical electrodes (Fig. 1) that can simulate the collective processes and nonlinear transverse dynamics of an intense beam propagating through a quadrupole lattice in a compact and flexible laboratory setup. Several important beam physics topics, such as beam mismatch, beam halo generation, collective mode excitation and control, adiabatic compression [9], and random noise effects [10], are also studied in PTSX. To perform these experimental studies, it is important to have a well-characterized initial beam [11]. In the present study, it is shown that an optimum ion injection process is critical for achieving such an initial beam state. Hence, the present paper concentrates on injection optimization by considering various factors, such as initial mismatch, production of high-energy particles, and two-stream interactions.

II. PAUL TRAP SIMULATOR EXPERIMENT (PTSX)

The PTSX device, cesium ion source, and diagnostics have been described in detail elsewhere [7,12] and only a brief summary is given here. To generate the oscillating quadrupole electric field, the PTSX device is composed of cylindrical electrodes of radius $r_w = 10$ cm that are sliced into four 90° azimuthal sectors. The central electrodes have length $2L = 2$ m while the end electrodes are each 40 cm long. The trap confines nonneutral ion plasmas radially by applying a periodic voltage $\pm V_0(t)$ with frequency f to the four sectors of the central electrode, creating a ponderomotive force that is directed radially inwards. A DC voltage $+\hat{V}$, which provides an axial potential well, is applied to the end electrodes. The

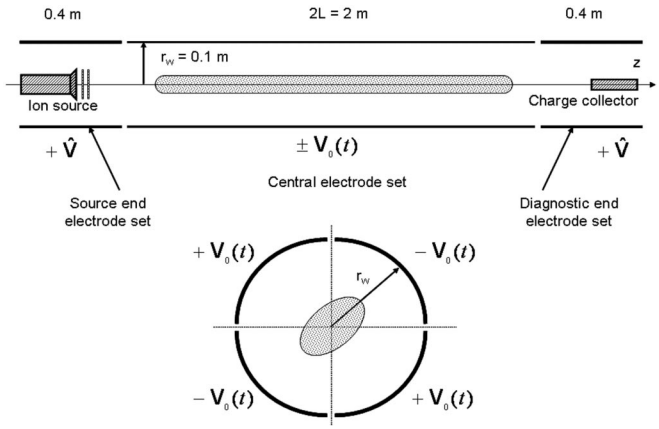

FIG. 1. Schematic of the PTSX device showing the quadrupole electrodes, ion source, and charge collector.

PTSX device manipulates the plasma using an inject-trap-dump cycle, and the one-component plasmas created in the trap are highly reproducible. During injection, the short electrodes on the source end are made to oscillate with the same voltage waveform as the central electrodes. The injection time is several milliseconds in order to allow cesium ions with several eV of kinetic energy to fill the trap. After injection is finished, the source end electrodes are switched from the fully oscillating voltage waveform to their static bias voltage. Finally, a long (~ 2 m) nonneutral ion plasma column is formed between the positively biased end electrodes. The typical operating pressure and ion number density in PTSX are 5×10^{-9} Torr and 1×10^5 cm^{-3}, respectively, and the plasma is collisionless to very good approximation.

III. MINIMIZATION OF INJECTION MISMATCH

The beam physics experiments performed on PTSX must begin with a nonneutral ion plasma column that corresponds to a matched beam so that the initial state is well known and characterized. However, during the injection stage, there can be a mismatch between the plasma emitted from the ion source and the transverse focusing lattice created by the applied voltage waveform. This mismatch can induce envelope oscillations, emittance growth, halo particles, and finally cause the trapped plasmas to have radial profiles far from those of thermal equilibrium states [1,2]. Because the ions are injected from the ion source with a circular, stationary cross section into a transverse focusing system in which the matched state has a pulsating elliptical beam envelope, the injected plasma column is always mismatched to the focusing lattice. This type of mismatch is inherent and unavoidable with the ion source as presently configured.

However, it is important to note that the injection mismatch can be minimized by adjusting the envelope of the plasma column to be as close as possible to the cross section of the ion source. If we apply the smooth-focusing approximation [1], a matched beam envelope can be effectively represented by a circular envelope with root-mean-square (rms) radius R_b. Further, if we consider an equivalent uniform density beam with outer radius $r_b = \sqrt{2}R_b$, then the transverse motion of the beam envelope evolves according to [1,2,13]

$$\frac{d^2 r_b}{dt^2} + \omega_q^2 r_b - \frac{\epsilon^2}{r_b^3} - \frac{K}{r_b} = 0, \tag{1}$$

where ω_q is the smooth-focusing frequency, $\epsilon = 2R_b[(2T_\perp/m) - (dR_b/dt)^2]^{1/2}$ is the unnormalized transverse emittance, $K = 2N_b q^2/4\pi\epsilon_0 m$ is the effective self-field perveance, and N_b is the line density. The effective transverse temperature $T_\perp = (2\pi/N_b) \times \int_0^{r_w} drrm\langle v_\perp^2\rangle n_b(r)/2$ measures the average kinetic energy associated with the random transverse motion of the beam particles, where the angular bracket $\langle \cdots \rangle$ denotes statistical average over the distribution function in transverse velocity space, and $n_b(r)$ is the density profile of the beam. Suppose that the ion source injects a uniform density plasma with transverse emittance ϵ_s and perveance K_s, then initially there can be an envelope oscillation around $\bar{r}_b = [(K_s + \sqrt{K_s^2 + 4\epsilon_s^2\omega_q^2})/2\omega_q^2]^{1/2}$. If the ion source radius r_s is equal to $\bar{r}_b$, then the envelope oscillation and injection mismatch can be minimized. The injection mismatch strength can be measured by the mismatch parameter $\mu = r_s/\bar{r}_b$, which is the ratio of the size of the initial beam to that of the matched beam [13]. For a matched beam, $\mu = 1$. We can adjust $\bar{r}_b$ by changing ω_q, K_s (or equivalently N_b), and ϵ_s. Changing $\epsilon_s \approx \sqrt{2}r_s(2T_s/m)^{1/2}$ requires controlling the temperature of the emission surface of the ion source T_s, which is not practical in the actual experiments. Therefore, most of the experiments on minimizing injection mismatch have been carried out by changing ω_q and N_b. For an applied voltage waveform $V_0(t) = V_{0\max}\sin(2\pi ft)$, the smooth-focusing frequency is given approximately by [7]

$$\omega_q = \frac{8qV_{0\max}}{m\pi r_w^2 f}\frac{1}{2\sqrt{2}\pi}. \tag{2}$$

Therefore, by changing $V_{0\max}$ and f, we can increase or decrease ω_q accordingly. However, due to the electronic limitations in generating the voltage waveform in the PTSX device, and the single-particle stability condition in the smooth-focusing vacuum phase advance $\sigma_v^{sf} = \omega_q/f < 115.6°$ [1], we can only increase ω_q up to about 90 kHz. On the other hand, the initial N_b can be controlled easily by adjusting the voltages on the emitter surface (V_s), acceleration grid (V_a), and deceleration grid (V_d) of the ion source. Normally, we set $V_s > V_a > V_d \geq 0$ V to avoid possible formation of a virtual cathode in the ion source region [2,14]. The voltage difference between the emitter surface and acceleration grid determines the extraction voltage V_e, and the voltage difference between the emitter surface and the deceleration grid adjusts the axial beam velocity v_b. The axial beam velocity remains almost constant throughout the trap and can be estimated from energy conservation. If we assume space-charge-limited current flow, then line density can be approximated by $N_b \approx I_{\rm CL}/qv_b \propto V_e^{3/2}$, where $I_{\rm CL}$ is the Child-Langmuir current.

The smooth-focusing injection mismatch is observed in experiments in which the extraction voltage is high enough that $\bar{r}_b$ is larger than r_s, i.e., when $\mu < 1$. To best measure this effect by minimizing the relaxation of the plasma to an equilibrium radial profile, PTSX is operated in a single-pass mode where the confining electrodes at the diagnostic end of the device do not trap the plasma axially. Ions travel from the ion source to the diagnostic in a single transit of the machine. For the experimental data on single-pass operation, each data point is obtained after averaging

over 100 repeated measurements, and the relative error is only a few percent.

The experimental data and 3D WARP particle-in-cell (PIC) simulation [15] results in Fig. 2 show the z-integrated radial current profile for the case where $\omega_q = 52.2$ kHz, $\sigma_v^{sf} = 49.8°$, and the extraction voltage is $V_e = 7.5$ V. The ion source injects enough ions to create a plasma that, when trapped, corresponds to a normalized density $s = \omega_p^2/2\omega_q^2 \sim 0.6$. Here, $\omega_p = (\hat{n}_b q^2/\epsilon_0 m)^{1/2}$ is the plasma frequency of the beam ions with on-axis density $\hat{n}_b$. If we take source parameters corresponding to $T_s \sim 0.1$ eV and $r_s = 0.762$ cm, then $\bar{r}_b = 1.6$ cm and $\mu = 0.48$. Hence, in this case, we expect a large initial mismatch. Shoulders in the radial profiles around $r = 3$ cm are observed in both the experiments and the simulations. This is the result of the initial mismatch. The radial position of the shoulder scales with ω_q as shown in Fig. 3; when ω_q is decreased, the shoulder moves outwards, and when ω_q is increased the shoulder moves towards the axis, or disappears. These types of radial profiles induced by beam mismatch were reported previously by Allen *et al.* [16]. This mismatch, when the plasma is trapped, causes the plasmas to have radial profiles with super-Gaussian tails.

The detailed structure of the initial mismatch can be seen in 3D WARP simulations (Fig. 4). In the single-pass mode, the time evolution of the beam envelope is mapped onto a z-varying beam envelope because $z \simeq v_b t$, and the axial coupling of the ion motion is small. The simulation results in Fig. 4 show that, near the ion source at $z = 0$, the initial mismatch appears as large-amplitude envelope oscillations at both the applied frequency f and the breathing-mode frequency ω_b. This breathing-mode frequency ω_b can be calculated from Eq. (1) to be

$$\omega_b^2 = 4\omega_q^2 - \frac{2K_s}{\bar{r}_b^2}. \tag{3}$$

The particle distribution relaxes as the injected particles move downstream, and when $z > 1$ m, the transverse density profile of the plasma consists of a core that oscillates with frequency ω_b, and exhibits a broad diffuse halo. This halo is produced by the combined effects of particle-core

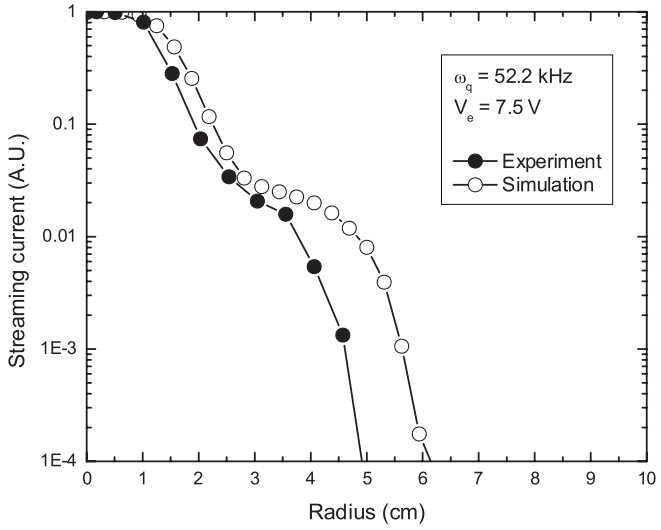

FIG. 2. The radial profile of the axial current streaming from the ion source to the charge collector in a single pass. Both experiment (solid circles) and simulation (open circles) show a shoulder around $r = 3$ cm.

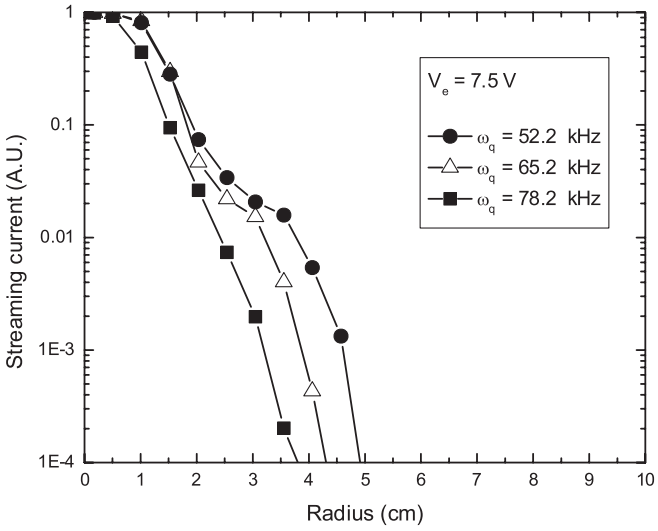

FIG. 3. Radial profiles of the axial streaming currents for several different smooth-focusing frequencies with fixed extraction voltage $V_e = 7.5$ V.

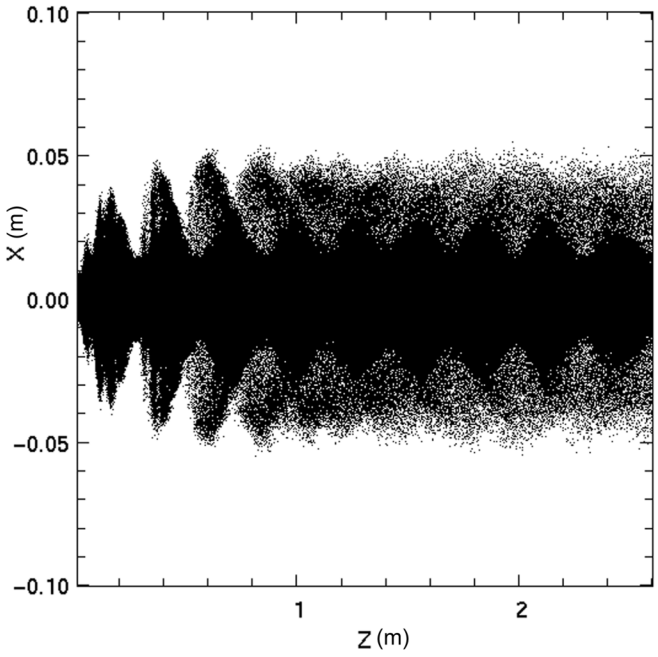

FIG. 4. 3D WARP PIC simulation of injection mismatch with $\omega_q = 52.2$ kHz and $V_e = 7.5$ V, showing both rapid and slow oscillations near $z = 0$ m. For larger z, the envelope oscillations result in a diffuse halo around the core.

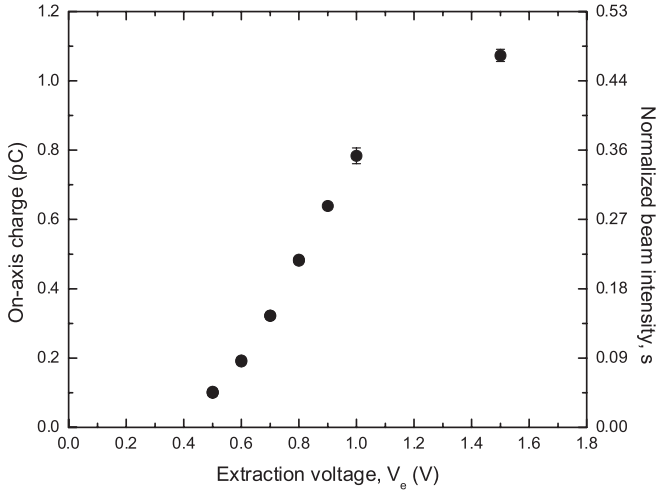

FIG. 5. On-axis charge dependence on the extraction voltage V_e for $V_s = 3$ V and $V_d = 0$ V.

resonance due to mismatch oscillations [13] and the finite spread in the axial velocity of the beam particles. The axial wavelength of the core oscillation is estimated to be $\lambda \sim v_b(2\pi/\omega_b)$, which gives $\lambda \sim 0.29$ m when $V_s = 9$ V, $V_d = 0$ V, $v_b = \sqrt{2q(V_s - V_d)/m} = 3615$ m/s, and $\omega_b = 77.7$ kHz. This wavelength is consistent with the simulation results, where there are about nine core envelope oscillations during the 2.6 m transit.

The simplest way to minimize the injection mismatch is to inject less plasma by decreasing the extraction voltage for a given axial beam velocity, so that the expected equilibrium radius of the plasma is nearly equal to the radius of the ion source. Figure 5 shows that the amount of charge injected can be easily adjusted by controlling the extraction voltage. When a plasma with moderately low space-charge density is well matched to the focusing channel, its radial profile becomes a nearly Gaussian profile shape, which corresponds to a straight line in the log versus r^2 plot [1]. After scanning the acceleration grid voltages, it is found that well-matched plasmas in the single-pass mode can be created with an extraction voltage of $V_e = 0.8$ V (Fig. 6). Here, the ion source bias voltage V_s has been lowered from 9 to 3 V to avoid possible two-stream interactions (discussed in Sec. V). These plasmas, when trapped, correspond to a normalized intensity of $s = 0.2$–0.3, and serve as the baseline case for subsequent experiments.

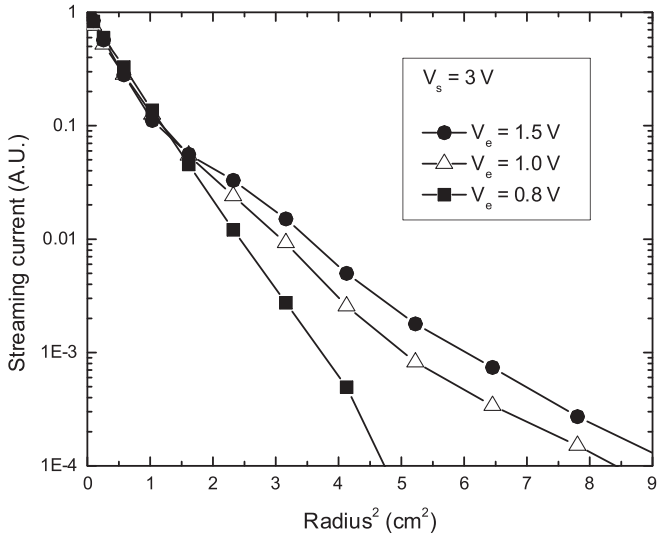

FIG. 6. Radial profiles of the axial streaming currents for several different extraction voltages with $V_s = 3$ V and $\omega_q = 52.2$ kHz. A straight line in the log versus r^2 plot indicates that the radial profile is a Gaussian.

IV. MINIMIZATION OF HIGH-ENERGY PARTICLES

In order to create well-matched one-component plasmas in PTSX, further optimization is required in addition to minimizing the initial mismatch. Experiments show that it is optimal to inject plasma for slightly less than the round-trip transit time of ions in the trap and to stop the ion emission a short time before closing the injection electrodes. Both considerations arise out of the need to minimize the number of particles present in the vicinity of the injection electrodes when the electrodes are switched from the fully oscillating voltage waveform to their static trapping voltage value $\hat{V}$. Ions that are near the injection region at the time the end electrodes close are increased to a potential energy as high as $q\hat{V}$. These high-energy particles can stream along the length of the trap, and then be reflected off the end potential of the trap with large excursions. Some of these high-energy particles may escape over the potential barrier on the dumping end and be detected by the charge collector. The result, whether the high-energy particles are trapped or not, is an unwanted distortion of the measured radial density profile.

Inhibiting ion emission with a bias voltage applied to the emission surface allows the already-injected ions to move away from the injection region. A simple ion source pulsing circuit has been installed for this purpose, which switches the voltage of the emitter surface to a negative bias at a short time Δt_i before the end of the injection stage. Keeping the total time duration of injection (t_i) less than a round-trip transit time of the ions (τ_b) minimizes the number of ions that have come back to the injection region. The round-trip transit time of an ion is estimated to be $\tau_b \approx 2 \times 2L/v_b \approx 1.92$ ms for the injection conditions in the previous section.

The data in Fig. 7 demonstrate that if Δt_i is at least 0.2 ms then the number of ions that overcome the axial potential barrier is minimized. If Δt_i is less than 0.2 ms, then high-energy particles can escape from the trap and be collected even when the dumping electrodes are not opened. The data in Fig. 8 indicate that the number of ions that pass over the axial trapping potential increases if

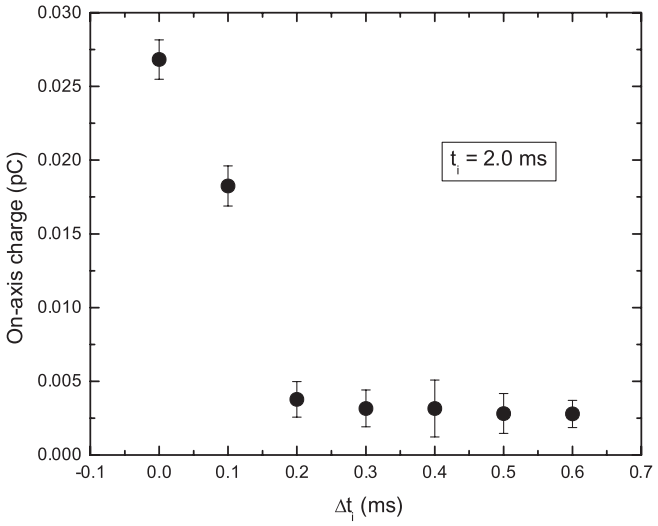

FIG. 7. On-axis charge dependence on Δt_i. By measuring the on-axis charge with the dumping electrode closed, one can effectively monitor the high-energy particles. Only ions with large kinetic energy $\gtrsim q\hat{V}$ can escape from the trap and be collected when the dumping electrodes are closed.

t_i is greater than about 1.9 ms. This is consistent with the estimate of the round-trip transit time of $\tau_b \sim 1.92$ ms. Therefore, for injection optimization, t_i is chosen to be 1.7 ms, and Δt_i is chosen to be 0.3 ms. If Δt_i is too large, the trapped plasma becomes bunched axially.

After injection is finished, the plasma is allowed to relax for several milliseconds. This relaxation time allows the residual mismatch oscillations to be damped away. As shown in Fig. 9, the relaxation time is approximately 6 ms. The radial density profile of the trapped plasma after 12 ms becomes nearly Gaussian [Fig. 10(A)], as expected for a thermal equilibrium distribution corresponding to moderately low space-charge density [1]. It is interesting

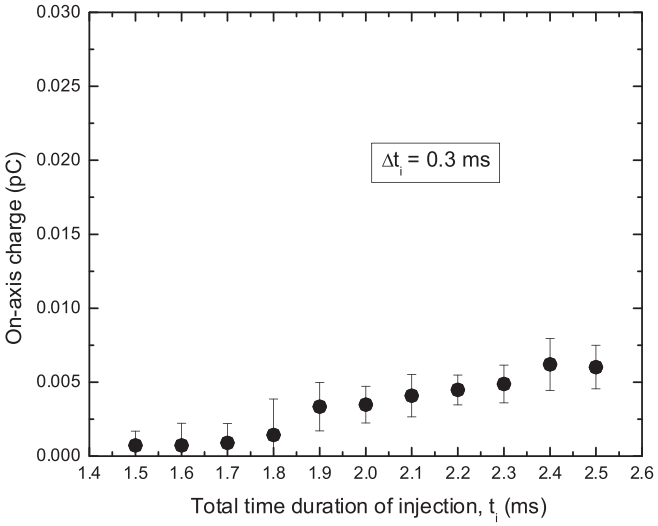

FIG. 8. On-axis charge dependence on the total time duration of injection t_i, for the optimum value of $\Delta t_i = 0.3$ ms.

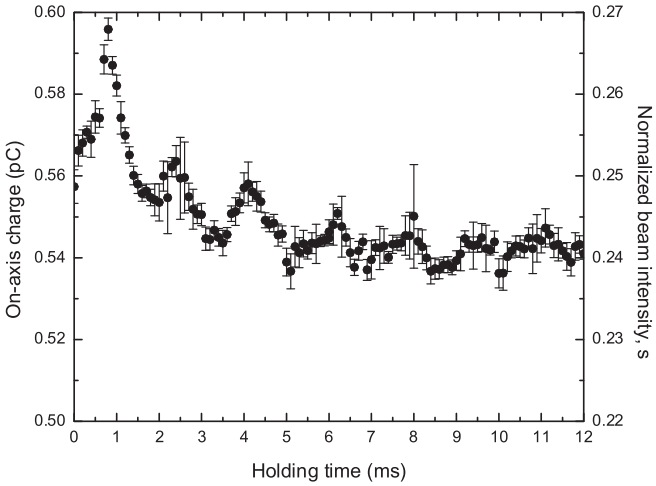

FIG. 9. Time history plot of on-axis charge after trapping with optimum injection conditions. After about 6 ms, the normalized beam intensity is about $s \sim 0.24$. The small residual oscillation in Fig. 9 has the period of the round-trip transit time of the beam ions in the trap.

to note that if we do not introduce the time delay Δt_i then the radial density profile has a super-Gaussian tail due to the presence of high-energy particles [Fig. 10(B)]. The rms radius $R_b = [(1/N_b)\int_0^{r_w} n_b(r) 2\pi r^3 dr]^{1/2}$ can be calculated from the measured radial density profile $n_b(r)$. For the case of $\Delta t_i = 0.3$ ms, R_b is calculated to be 0.85 cm. On the other hand, for $\Delta t_i = 0.0$ ms, R_b has increased to 1.38 cm. Therefore, minimization of the population of high-energy particle is very important in establishing a well-behaved beam equilibrium. For a thermal equilibrium distribution, the global force balance equation can be

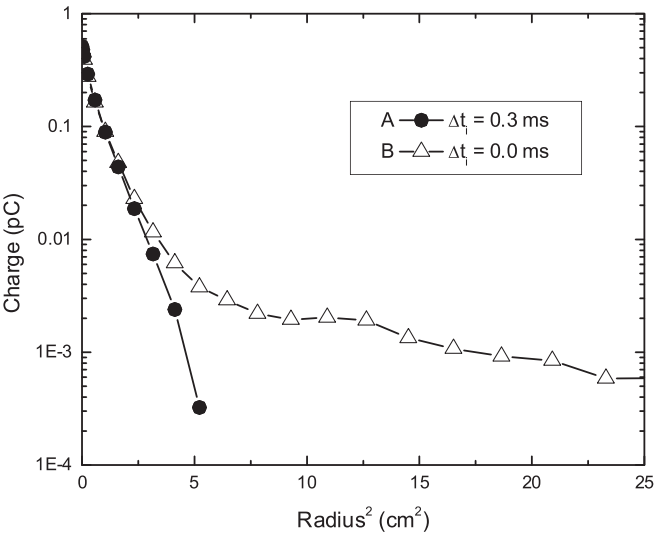

FIG. 10. Measured radial profiles of the trapped plasmas with $\omega_q = 52.2$ kHz: after minimizing the population of high-energy particles (A); and with a significant population of high-energy particles (B). A straight line in the log versus r^2 plot indicates that the radial profile is a Gaussian.

written as [1]

$$m\omega_q^2 R_b^2 = 2T_\perp + \frac{N_b q^2}{4\pi\epsilon_0}. \quad (4)$$

The transverse temperature inferred from the global force balance equation (4) is $T_\perp = 0.13$ eV for the trapped plasma with $\Delta t_i = 0.3$ ms, which is consistent with the thermal temperature of the cesium ion source ($\sim 1000\,^\circ$C).

V. TWO-STREAM INTERACTIONS

During the injection stage, the stream of ions leaving the ion source interacts with the counterstreaming ions that have reflected off the end of the trap. In these counterstreaming plasmas, two-stream interactions may be a source of noise in the signal, and may deteriorate the beam quality [14,17]. From the analysis of the appropriate dispersion relation and 3D WARP simulations, it is found that there is a threshold value of normalized intensity for the onset of instability, and the beam remains quiescent during the injection stage and the early stage of trapping for the experimental conditions described in the previous two sections. Therefore, we conclude that two-stream interactions are not a large concern during the injection stage if we inject beams with moderately low space-charge density ($s = 0.2$–0.3). However, if we hold the plasma longer for many bounce periods inside the axial potential barrier, then eventually two-stream interactions will begin to develop due to the perturbations in the vicinity of the turning points. Near the turning points, the local density is much higher than in the trap, resulting in enhanced two-stream interactions and beam bunching [14].

We consider a simplified model in which a uniform density ion beam with directed axial velocity $+v_b$ and number density $\hat{n}_b/2$ is propagating through another symmetric, counterstreaming beam with directed axial velocity $-v_b$ and number density $\hat{n}_b/2$. For analytical simplicity, both beam components are assumed to have Lorentzian distributions in axial velocity v_z with identical effective thermal speed $v_{T\|} = (2T_\|/m)^{1/2}$. With these assumptions, the dispersion relation for dipole-mode perturbations is given by [1,18]

$$1 = \frac{\omega_p^2/4}{[(\omega - k_z v_b + i|k_z|v_{T\|})^2 - \nu^2]} + \frac{\omega_p^2/4}{[(\omega + k_z v_b + i|k_z|v_{T\|})^2 - \nu^2]}. \quad (5)$$

Here, ω and k_z are the complex oscillation frequency and axial wave number of the perturbations with azimuthal mode number $l = 1$, corresponding to a simple (dipole) transverse displacement of two counterstreaming ion beams. We also introduce the depressed betatron frequency-squared defined by $\nu^2 = \omega_q^2 - \omega_p^2/2 = \omega_q^2(1 - s)$. The condition for the instability ($\mathrm{Im}\,\omega > 0$) can be expressed in terms of the threshold value of normalized intensity s_{th} as

$$s > s_{\mathrm{th}} = 4\frac{v_b/v_{T\|}}{(1 + v_b/v_{T\|})^2}, \quad (6)$$

for $v_b > v_{T\|}$. Note that $s < 1$ is required for transverse confinement of the beam ions [3]. From 3D WARP simulations, it is found that longitudinal cooling of the parallel temperature $T_\|$ due to acceleration [2] is weak and $T_\|$ remains the same order as the source temperature $T_s \sim 0.1$ eV. If we take the experimental parameters to be $T_\| \approx T_s \sim 0.1$ eV, $V_s = 3$ V, and $V_d = 0$ V, then $v_b = 2087$ m/s, $v_{T\|} = 381$ m/s, and $s_{\mathrm{th}} = 0.53$. Hence, two-stream interactions for beams with $s = 0.2$–0.3 are expected to be stable as long as $s < s_{\mathrm{th}}$, which may not be true near the end turning points of the trap.

The phase-space plot in Fig. 11 shows that the main stream of the beam remains quiescent after injection with $|v_b|$ around 2000 m/s and finite velocity spread, both of which are consistent with simple estimations. Even though we choose experimental conditions to minimize the production of high-energy particles, there still exist some high-energy particles, with maximum velocity estimated by $v_{z\,\max} \approx [2q(V_s - V_d + \hat{V})/m]^{1/2} \approx 7525$ m/s for $\hat{V} = 36$ V. The gap in the middle of the downstream beam is a result of introducing the time delay Δt_i. On the other hand, if we hold the plasma longer (> 10 ms) inside the trap, the two-stream interactions become stronger (Fig. 12), which may be associated with the fluctuations due to local density buildup near the turning points at the

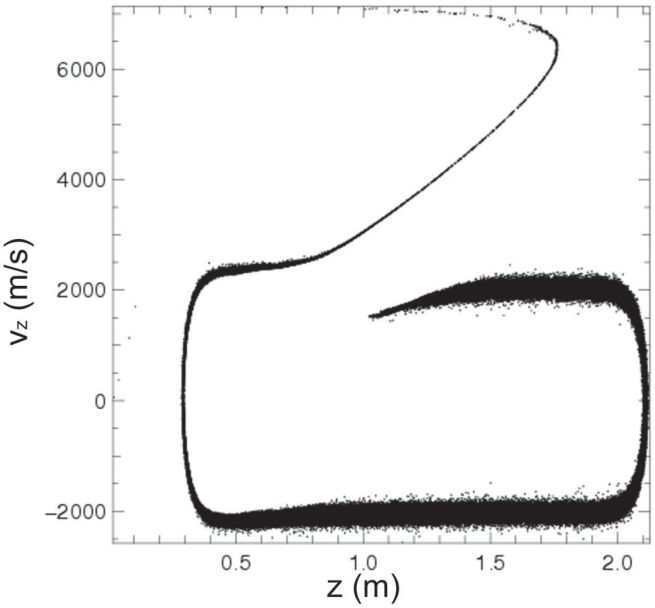

FIG. 11. 3D WARP simulation results for $\omega_q = 52.2$ kHz for the injection conditions summarized in the text. Plot of axial (z, v_z) phase space at 0.3 ms after closing the injection electrodes.

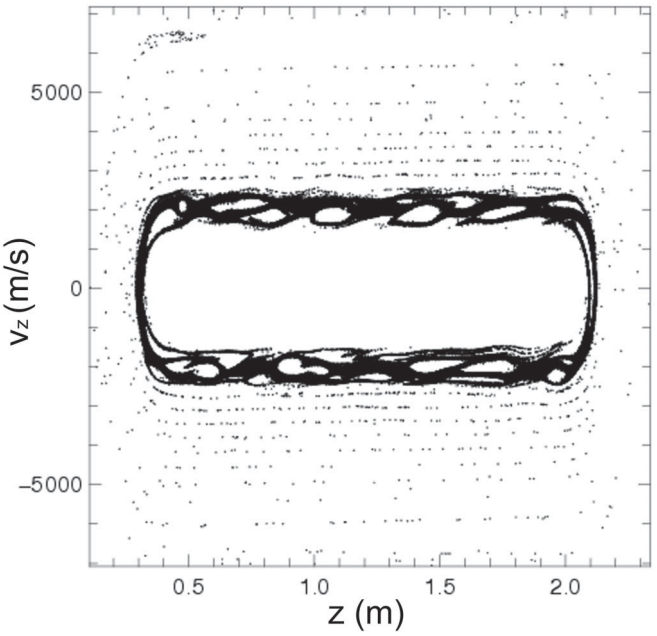

FIG. 12. 3D WARP simulation results for $\omega_q = 52.2$ kHz for the injection conditions summarized in the text. Plot of axial (z, v_z) phase space at 13 ms after closing the injection electrodes.

end of the trap. These two-stream interactions mix the multistreaming beams inside the trap and increase the longitudinal temperature. The effects of two-stream interactions on the transverse dynamics of the trapped ions are undergoing further study using 3D WARP simulations. As mentioned earlier, the purpose of the PTSX device is to simulate the transverse dynamics of a continuous beam propagating in kilometer-long periodic-focusing transport lines. In this regard, it is important that the trapped plasma be maintained at least several tens of milliseconds without significant distortion of the radial profiles. For the case of beams with moderately low space-charge density and axial beam velocity, the effects of two-stream interactions on the transverse confinement after a long holding time turn out to be small. In the experimental results reported previously [7], it was shown that a plasma with moderate space-charge intensity is maintained over 300 msec with only slight degradation in the density profile. The phase-space plot in Fig. 12 also indicates that a small but finite number of high-energy particles still remain inside the trap along with the main beam ions even after a long holding time.

VI. SUMMARY

In summary, the optimum ion injection conditions have been determined for the PTSX device. By reducing the amount of charge injected, and by optimal timing of the injection and trapping of the plasma, a well-matched initial plasma is formed inside the trap. This initial plasma is used as the baseline for various beam physics experiments of current interest [11]. Two-stream interactions are shown to be relatively weak during the injection stage, but can affect beam quality after a sufficiently long holding time. The injection optimization process reported in this paper can be useful for other similar ion [6,8,19] or electron [14] trap devices.

ACKNOWLEDGMENTS

This research was supported by the U.S. Department of Energy. The authors would like to thank Mr. A. Carpe for his excellent technical support, and Dr. D. P. Grote and Dr. E. A. Startsev for useful discussions regarding the WARP simulations.

[1] R. C. Davidson and H. Qin, *Physics of Intense Charged Particle Beams in High Energy Accelerators* (World Scientific, Singapore, 2001).
[2] M. Reiser, *Theory and Design of Charged Particle Beams* (Wiley, New York, 1994).
[3] R. C. Davidson, H. Qin, and G. Shvets, Phys. Plasmas **7**, 1020 (2000).
[4] H. Okamoto and H. Tanaka, Nucl. Instrum. Methods Phys. Res., Sect. A **437**, 178 (1999).
[5] N. Kjærgaard and M. Drewsen, Phys. Plasmas **8**, 1371 (2001).
[6] N. Kjærgaard, K. Mølhave, and M. Drewsen, Phys. Rev. E **66**, 015401(R) (2002).
[7] E. P. Gilson, R. C. Davidson, P. C. Efthimion, and R. Majeski, Phys. Rev. Lett. **92**, 155002 (2004).
[8] R. Takai, K. Ito, Y. Iwashita, H. Okamoto, S. Taniguchi, and Y. Tomita, Nucl. Instrum. Methods Phys. Res., Sect. A **532**, 508 (2004).
[9] M. Dorf, R. C. Davidson, and E. A. Startsev, Phys. Rev. ST Accel. Beams **9**, 034202 (2006).
[10] C. L. Bohn and I. V. Sideris, Phys. Rev. Lett. **91**, 264801 (2003).
[11] E. P. Gilson, M. Chung, R. C. Davidson, M. Dorf, P. C. Efthimion, D. P. Grote, R. Majeski, and E. A. Startsev, Nucl. Instrum. Methods Phys. Res., Sect. A (to be published).
[12] E. P. Gilson, M. Chung, R. C. Davidson, P. C. Efthimion, R. Majeski, and E. A. Startsev, Nucl. Instrum. Methods Phys. Res., Sect. A **544**, 171 (2005).
[13] T. P. Wangler, K. R. Crandall, R. Ryne, and T. S. Wang, Phys. Rev. ST Accel. Beams **1**, 084201 (1998).
[14] V. Gorgadze, T. A. Pasquini, J. Fajans, and J. S. Wurtele, *Non-Neutral Plasma Physics V: Workshop on Non-Neutral Plasmas*, AIP Conf. Proc. No. 692 (American Institute of Physics, New York, 2003), p. 30.
[15] A. Friedman, D. P. Grote, and I. Haber, Phys. Fluids B **4**, 2203 (1992).
[16] C. K. Allen *et al.*, Phys. Rev. Lett. **89**, 214802 (2002).
[17] T. H. Stix, *Waves in Plasmas* (American Institute of Physics, New York, 1992).
[18] R. C. Davidson, H. Qin, P. H. Stoltz, and T. S. Wang, Phys. Rev. ST Accel. Beams **2**, 054401 (1999).
[19] G. Savard, Nucl. Instrum. Methods Phys. Res., Sect. B **126**, 361 (1997).